ARCHIVES OF CIVIL AND MECHANICAL ENGINEERING 17 (2017) 55–64

Available online at www.sciencedirect.com

ScienceDirect

journal homepage: http://www.elsevier.com/locate/acme

Original Research Article

Thermal and mechanical properties of sustainable lightweight strain hardening geopolymer composites

Behzad Nematollahi[a,*], *Ravi Ranade*[b], *Jay Sanjayan*[a], *Sayanthan Ramakrishnan*[a]

[a] *Center for Sustainable Infrastructure, School of Engineering, Faculty of Science, Engineering and Technology, Swinburne University of Technology, Melbourne, Victoria, Australia*

[b] *Department of Civil, Structural, and Environmental Engineering, State University of New York, Buffalo, NY 14260-4300, USA*

ARTICLE INFO

Article history:
Received 17 March 2016
Accepted 13 August 2016
Available online

Keywords:
Tensile strain hardening
Engineered geopolymer composite
Engineered cementitious composite
Lightweight concrete
Thermal conductivity

ABSTRACT

The thermal and mechanical properties of sustainable lightweight engineered geopolymer composites (EGCs), exhibiting strain-hardening behavior under uniaxial tension, are reported in this study. Fly ash-based geopolymer was used as complete replacement of cement binder to significantly increase the environmental sustainability of the composite compared to the engineered cementitious composite (ECC). Additionally, three types of lightweight aggregates including expanded perlite, microscopic hollow ceramic spheres and expanded recycled glass were used as complete replacement of micro-silica sand to reduce density and thermal conductivity of the composite. The influences of the type of aggregates on the fresh and hardened properties of the composite including matrix workability, density, compressive strength, thermal conductivity and uniaxial tensile performance were experimentally evaluated. The results indicated that the density and compressive strength of all EGCs developed in this study, even the EGC containing normal weight micro-silica sand, were less than 1833 kg/m^3 and more than 43.4 MPa, respectively, meeting the density and compressive strength requirements for structural lightweight concrete. Replacing normal weight micro-silica sand with lightweight aggregates reduced the compressive and tensile strengths of the EGCs by a maximum of 24% and 32%, respectively. However, the tensile ductility of the EGCs containing lightweight aggregates was comparable to that of the EGC containing micro-silica sand. In addition, the thermal conductivity of the EGCs containing lightweight aggregates were significantly (38–49%) lower than that of the EGC containing normal weight micro-silica sand, resulting in an end-product that is greener, lighter, and provides better thermal insulation than ECC.

* *Corresponding author at*: Swinburne University of Technology, Mail 38, PO Box 218, FSET, Hawthorn, Victoria 3122, Australia.
E-mail address: bnematollahi@swin.edu.au (B. Nematollahi).

http://dx.doi.org/10.1016/j.acme.2016.08.002

1. Introduction

In the construction industry, the use of lightweight concrete (with a density less than 1850 kg/m^3 [1]) instead of normal weight concrete (2400 kg/m^3) is favorable as it offers several advantages such as reduction in dead loads and section dimensions, enhanced thermal insulation, savings in steel reinforcement, ease of handling and transportation, and lower overall cost [2]. However, one of the major disadvantages of lightweight concrete is greater brittleness and lower fracture toughness compared to normal weight concrete of similar compressive strength [2,3]. For instance, Hengst and Tressler [4] reported that the fracture energy of lightweight foam concrete was significantly lower than that of normal weight concrete. According to Zhang and Gjvorv [5], the tensile to compressive strength ratio of high strength lightweight concrete was lower than that of high strength normal weight concrete. This is attributed to the use of lightweight aggregates, which are usually weaker than the cement matrix, which makes them susceptible to cracking [3]. In past studies, different fibers have been introduced in the mixture design of lightweight concrete to enhance its tensile and flexural strengths, and the flexural toughness. However, these fiber-reinforced lightweight concretes, similar to conventional fiber-reinforced concrete, exhibit tension softening behavior [6,7]. Thus, although the lower density of lightweight concrete promotes its application as an alternative to normal weight concrete, the low tensile ductility and fracture toughness hinder the widespread structural applications of lightweight concrete in the construction industry.

Engineered cementitious composite (ECC) is a special class of high performance fiber reinforced cementitious composites (HPFRCCs) which exhibits strain hardening behavior under tension with very high tensile ductility [8]. The average density, compressive and tensile strengths, and tensile strain capacity of typical PVA-ECC mix 45 (M45) are about 2077 kg/m^3, 52.6 MPa, 6 MPa and 2.7%, respectively, at the age of 28 days [9]. Thus, the tensile ductility of typical ECC M45 is several hundred times the ductility of conventional concrete in tension. Several studies have been conducted to investigate the application of ECC in shear elements subjected to cyclic loading, in mechanical fuse elements in beam-column connections, in shear wall retrofitting of reinforced concrete (RC) buildings, in RC beams as durable cover for rebar corrosion control, and in general concrete structural repair. Other potential applications of ECC are in high-energy absorption structures including short columns, dampers, and connections for hybrid steel/RC structures [10].

Although the density of typical ECC M45 is lower than that of normal weight concrete (2400 kg/m^3), it cannot be considered lightweight according to the definition of ACI Committee 213, which requires the density of concrete at 28 days to be less than 1850 kg/m^3 to qualify as lightweight concrete [1]. Wang and Li [3] attempted to develop lightweight ECCs using four lightweight fillers including expanded perlite, hollow glass bubbles, polymeric microform, and air bubbles produced by air entrainment admixture. In that study, it was found that hollow glass bubbles were effective for lowering the density and improving the fiber dispersion and mechanical properties of ECC [3]. The average density, compressive and tensile strengths, and tensile strain capacity of 1450 kg/m^3, 41.7 MPa, 4.31 MPa and 4.24%, respectively, were reported for the lightweight ECC made by hollow glass bubbles with a mean size of 30 μm [3]. However, such lightweight ECC uses high amount of cement and high temperature-processed hollow glass bubbles [3], which results in high embodied energy and carbon footprint [11], lowering the environmental sustainability of the composite. Therefore, it is necessary to develop green and sustainable lightweight ECCs with significantly lower environmental footprints.

This study evaluates the mechanical and thermal properties of green lightweight engineered geopolymer composites (EGCs) incorporating fly ash-based geopolymer as complete replacement of ordinary Portland cement (OPC) and three types of lightweight aggregates including expanded perlite, microscopic hollow ceramic spheres and expanded recycled glass as complete replacement of micro-silica sand, to achieve the following three objectives: (1) to significantly reduce the environmental footprint, (2) to decrease the density of the composite, and (3) to reduce the thermal conductivity of the composite. These objectives need to be achieved while maintaining good workability of fresh matrix and reasonable strength. A series of experiments including workability of the fresh matrix, density, compression, thermal conductivity and uniaxial tension tests were conducted as detailed in the following sections to characterize the thermal and mechanical properties of the developed green lightweight EGCs.

Among the ingredients of ECC M45, cement is a major contributor to the environmental impact accounting for 48.2% and 81.6% of total embodied energy and CO_2 emissions, respectively [12]. Several studies have focused on replacing cement in ECC M45 with industrial wastes. For instance, normal weight green ECCs have been developed by partial replacement of cement with fly ash [9], slag [13] and iron ore tailings (IOTs) [12].

Recently, Huang et al. [11] attempted to achieve the properties of lightweight and material greenness in ECC, simultaneously. In that study, green lightweight ECCs (GLECCs) were produced using IOTs, fly ash, and fly ash cenosphere as aggregates, mineral admixture, and lightweight filler, respectively [11]. The density, compressive and tensile strengths, and tensile strain capacity in the range of 1649–1820 kg/m^3, 25.0–47.6 MPa, 4.8–5.9 MPa and 3.3–4.3%, respectively, were reported for the developed GLECCs at the age of 28 days, depending on the contents of IOTs, fly ash, and fly ash cenosphere [11]. In this study, lightweight EGC is developed, which is even more environmentally sustainable than the previously developed GLECCs, as the ordinary Portland cement (OPC) binder in ECC is completely replaced by fly ash-based geopolymer binder in EGC.

Fly ash-based geopolymer is a cement-less binder that provides a highly sustainable alternative to OPC [14]. The term geopolymer was firstly introduced by Davidovits [15] as a class of largely X-ray amorphous aluminosilicate binder materials [16]. Geopolymers can be synthesized at ambient or elevated temperature by alkali activation of industrial by-products such as fly ash and slag, which are rich in silica and alumina, or materials of geological origin such as metakaolin [14,17,18]. Previous studies reported that manufacture of fly ash-based

Table 1 – Chemical composition of fly ash, expanded recycled glass and hollow ceramic microspheres.

Chemical	Component (wt.%)		
	Fly ash	Expanded recycled glass[b]	Hollow ceramic microspheres[b]
Al_2O_3	25.56	2.5	30 – 36
SiO_2	51.11	71.7	55 – 65
CaO	4.3	8.9	–
Fe_2O_3	12.48	0.4	1 – 2
K_2O	0.7	0.8	–
MgO	1.45	2.1	–
Na_2O	0.77	13.2	–
P_2O_5	0.885	–	–
TiO_2	1.32	0.1	0.5 – 1.0
MnO	0.15	0.0	–
SO_3	0.24	0.1	–
LOI[a]	0.57	0.3	–

[a] Loss on ignition.
[b] The values are reported by the manufacturer.

geopolymer releases at least 80% less CO_2 and consumes around 60% less energy compared to production of OPC [19,20]. According to the U.S. Department of Energy [21], a major portion of the total energy consumption in buildings is associated with space heating and cooling. This energy demand can be significantly reduced by using construction materials with lower thermal conductivity (which means better insulating). Thus, using an EGC with lower thermal conductivity in a building will be highly sustainable not only in terms of material greenness but will also reduce the energy needs over the use phase of the building.

2. Experimental procedures

2.1. *Materials and mix proportions*

The low calcium fly ash (class F) used in this study was supplied from Gladstone power station in Queensland, Australia. Table 1 presents the chemical composition and loss on ignition (LOI) of the fly ash determined by X-ray fluorescence (XRF). The total does not sum up to 100% because of rounding errors. A sodium-based (Na-based) activator combination, composed of 8.0 M sodium hydroxide (NaOH) and D grade sodium silicate (Na_2SiO_3) solutions, was used in this study. Previous studies by the authors of this paper revealed that the use of Na-based activator combination composed of 8.0 M NaOH solution (28.6%, w/w) and Na_2SiO_3 solution (71.4%, w/w) with a SiO_2 to Na_2O ratio of 2.0 is highly beneficial in the production of fly ash-based EGCs [22–25]. NaOH solution was prepared with a concentration of 8.0 M using NaOH beads of 97% purity supplied by Sigma–Aldrich and tap water. The D grade Na_2SiO_3 solution was supplied by PQ Australia with a specific gravity of 1.51 and a modulus ratio (Ms) equal to 2.0 (where $Ms = SiO_2/Na_2O$, $Na_2O = 14.7\%$ and $SiO_2 = 29.4\%$). NaOH and Na_2SiO_3 solutions were mixed together with Na_2SiO_3/NaOH mass ratio of 2.5 to prepare the Na-based activator combination. Table 2 presents properties of the PVA fiber with a surface oil coating of 1.2% by weight, supplied by Kuraray Co. Ltd., Japan.

Washed and sieve-graded micro-silica sands with an average size of 165 μm, maximum size of 212 μm, and average specific gravity of 2.6 was supplied by TGS Industrial Sand Ltd., Australia. Reducing the composite density without sacrificing compressive and tensile strengths of the composite is one of the challenges of developing lightweight composites, since the weak lightweight aggregates act similar to flaws in the matrix [3]. From fracture mechanics, the largest existing flaw size determines the tensile strength of a brittle matrix such as geopolymer. However, the compressive strength is governed by a group of relatively large flaws [3]. Thus, in order to reduce the detrimental effect of using lightweight aggregates on the compressive and tensile strengths, Wang and Li [3] recommended that the particle size of the lightweight aggregates should be much smaller than the most common pre-existing flaws (i.e. entrapped air bubbles with sizes more than 1 mm) in the composite. On the other hand, using lightweight aggregates with small particle size is also beneficial with respect to the workability of the composite, since aggregates with large particle size have negative impact on fiber dispersion [3]. Therefore, three types of small-size lightweight aggregates, as complete replacement of micro-silica sand, with the same volume percentage were used in this study.

(1) Lightweight expanded glass aggregates with granular sizes in the range of 40–125 μm and specific gravity of 1.4 was supplied by Dennert Poraver GmbH, Germany. The expanded glass aggregates are industrially manufactured from post-consumer recycled glass. The chemical analysis of expanded recycled glass as reported by the manufacturer and determined by atomic emission spectrometric (AES) is also given in Table 1.
(2) Grade SL125 is a fine grade white hollow ceramic microspheres, supplied by Envirospheres Pty Ltd., Australia, which has granular sizes in the range of 12–125 μm. The average particle size and specific gravity of Grade SL125 microspheres are about 80 μm and 0.85, respectively. The typical chemical properties of hollow ceramic microspheres, as reported by the manufacturer, are also given in Table 1.
(3) Grade AP20 expanded perlite is an ultra-lightweight and inert non crystalline siliceous volcanic mineral aggregate, with average particle size and specific gravity of 43 μm and

Table 2 – Properties of PVA fiber.

Fiber type	Diameter (μm)	Length (mm)	Young's modulus (GPa)	Elongation (%)	Nominal strength (MPa)	Density (g/cm^3)
RECS 15×8	40	8	41	6	1600	1.3

Table 3 – Mix proportions of green lightweight fly ash-based EGCs.

Mix ID	Fly ash	Act.[a]	Aggregates				PVA fiber
			Silica sand	Expanded glass	Ceramic microsphere	Expanded perlite	
EGC-S	1.0 [1029.7]	0.45 [463.4]	0.30 [308.9]	–	–	–	0.02 [26]
EGC-G	1.0 [1073.3]	0.45 [483]	–	0.16 [171.7]	–	–	0.02 [26]
EGC-M	1.0 [1006.5]	0.45 [452.9]	–	–	0.10 [100.6]	–	0.02 [26]
EGC-P	1.0 [1220.9]	0.45 [549.4]	–	–	–	0.03 [36.6]	0.02 [26]

All numbers are mass ratios of fly ash weight except fiber content (volume fraction) and the numbers in brackets (amount of material per cubic meter (kg/m^3)).
[a] The Na-based activator combination.

0.293, respectively (supplied by Ausperl Pty Ltd., Australia). In Grade AP20 expanded perlite, 90% of particles are smaller than 87 μm.

Table 3 presents the four green lightweight fly ash-based EGC mix proportions investigated in this study. In all mixtures, the weight ratio of activator solution to fly ash was kept constant at 0.45, and volume fraction of the PVA fibers was fixed at 2%. In the mixture EGC-S, the weight ratio of micro-silica sand to fly ash was selected as 0.30. This dosage has been identified in the previous studies by the authors as the most suitable to promote optimum rheology and desirable mechanical properties in fly ash-based EGCs [26,27]. In the other three mixtures, the weight ratios of lightweight aggregates to fly ash were calculated to maintain the same volume percentage as that of the micro-silica sand in the mixture EGC-S.

2.2. *Mixing, curing and testing of specimens*

All mixtures were prepared in a 3 l Hobart mixer. To prepare the fly ash-based geopolymer matrix, fly ash and aggregates were dry mixed for about 1 min at low speed. Then, the alkaline solution was gradually added and the mixing was continued for about 4 min. After the matrix ingredients were thoroughly mixed to achieve the desired fresh state, the flowability of fresh geopolymer matrix (before addition of the fibers) was measured to ensure that the flowability was within the desired range for achieving good fiber dispersion. Finally, the PVA fibers (2% volume fraction) were gradually added to ensure uniform fiber dispersion. The whole mixing procedure for each mix generally took 15 min. The fresh geopolymer matrix and composite were cast into different molds and compacted using a vibrating table.

Heat curing was adopted in this study, based on the authors' previous research which indicated that the heat curing enhances both strength and ductility properties of the fly ash-based EGCs [22,23]. For heat curing, all molds were sealed to minimize moisture loss and were placed in an oven at 60 °C for 24 h. At the end of 24 h, the specimens were removed from the oven, kept undisturbed until being cool, and then de-molded and left in the laboratory at ambient temperature until the day of mechanical tests. All specimens were tested 3 days after casting. Previous studies have shown that, unlike cement-based materials, the age does not have considerable effect on the strength of geopolymers after the completion of the heat curing. Furthermore, three-day compressive strength of heat cured fly ash-based geopolymer is equivalent to a typical OPC strength development after 28-days [28,29].

To determine flowability of fresh geopolymer matrix, mini slump test also known as spread-flow test was conducted. Details of the mini-slump test can be found in Nematollahi and Sanjayan [30]. The relative slump value is derived from the following equation:

$$\Gamma_p = \left(\frac{d}{d_0}\right)^2 - 1 \quad (1)$$

where Γ_p is the relative slump, d is the average of two measured diameters of the matrix spread, and d_0 is the bottom diameter of the mini-slump cone equal to 100 mm in this study [31].

Compressive strength of each mix was measured according to ASTM C109 [32]. In this regard, for each mix at least three 50 mm cube specimens were cast and compacted using a vibrating table. The cube specimens for compressive strength tests were weighed on the testing day to determine the density of the composite. Uniaxial tension tests were conducted to evaluate the behavior of the developed green lightweight EGCs under tension. For each mix, at least three rectangular coupon specimens with the dimensions of 400 mm × 75 mm × 10 mm were prepared. All coupon specimens were tested in uniaxial tension under displacement control at the rate of 0.25 mm/min over a gauge length of about 80 mm. Further details of the uniaxial tension test can be found in Nematollahi et al. [22].

Thermal conductivity measurements were conducted on the same coupon specimens that were used for the uniaxial tension tests. In this regard, an un-cracked area of 75 mm × 75 mm of each coupon specimen located within the wedge grips during the uniaxial tension tests was cut for the thermal conductivity measurements. As most residential or commercial buildings are subjected to air drying, thermal conductivity measurements were undertaken under air-dry state in the laboratory environment similar to field exposure. In this regard, the cut coupon specimens were kept in the laboratory environment (23 ± 3 °C) for about a month and thermal conductivity measurements were then conducted using a TCi thermal conductivity analyzer. The TCi developed by C-Therm Technologies Ltd. is a device that measures the thermal conductivity of a small sample, by using the Modified Transient Plane Source (MTPS) method [33]. The experimental setup and data processing details can be found in Cha et al.

Table 4 – Workability, density and compressive strength results.

Mix ID	Matrix workability[a]	Density (kg/m^3)	Compressive strength (MPa)
EGC-S	8.8	1828 ± 16	56.8 ± 3.7
EGC-G	6.7	1754 ± 4	43.4 ± 2.4
EGC-M	7.4	1586 ± 6	46.8 ± 3.0
EGC-P	7.1	1833 ± 4	48.2 ± 3.2

[a] Relative slump value of the fresh matrix.

[33]. After the test, specimens were placed in an oven at 105 °C for 24 h to measure the moisture content.

3. Results and discussion

3.1. Workability and density

The fresh matrix workability of each mix is given in Table 4. It should be pointed out that the reported relative slump values are based on the mini-slump test without the 25 times tamping of the flow table. From visual observations, based on past experience of mixing ECC, all geopolymer matrices exhibited adequate workability and rheology to guarantee uniform fiber dispersion. As shown in Table 4, EGC-S and EGC-G exhibited the highest and lowest matrix workability, respectively. The relatively low matrix workability of EGC-G may be attributed to the high water absorption of expanded glass particles [34]. The matrix workability of EGC-G, EGC-M and EGC-P containing lightweight aggregates were 24%, 16% and 19% lower than that of EGC-S containing micro-silica sand, respectively.

The average density of each mix is presented in Table 4. The density of green lightweight EGCs was in the range of 1586–1833 kg/m^3, which is 24–34% less than that of a normal weight concrete with a density of 2400 kg/m^3 and meet the density requirement for lightweight concrete (below 1850 kg/m^3) [1]. It should be pointed out that even EGC-S containing normal weight micro-silica sand (typically used in ECC) exhibited an average density of 1828 kg/m^3, which can be classified as lightweight concrete. The density of EGC-S is 12% less than that of typical ECC M45 (2077 kg/m^3). This may be attributed to the lower specific density of fly ash (2.45 g/cm^3) than that of cement (3.15 g/cm^3). Therefore, replacing the OPC binder by fly ash-based geopolymer binder is beneficial for weight reduction of composite.

According to Table 4, the densities of EGC-G and EGC-M are 4% and 13%, respectively, lower than that of EGC-S. The densities of EGC-S and EGC-P are comparable. Among the lightweight aggregates, hollow ceramic microspheres were the most effective in reducing the density of the composite. This may be attributed to the hollow and closed shell structure and the low particle density of microsphere particles [35]. It should be noted that the density of the EGC-M mixture (1586 kg/m^3) developed in this study is lower than that of the lightest GLECCs (the mixture C6 with the average density of 1649 kg/m^3) developed by Huang et al. [11], where fly ash to cement ratio was 4.4 and micro-silica sand was completely replaced by fly ash cenosphere.

3.2. Compressive strength

The average compressive strength of each mix is also presented in Table 4. The compressive strength of green lightweight EGCs at 3 days after casting ranged from 43.4 MPa to 56.8 MPa, which is well above the compressive strength requirement of 17 MPa for structural lightweight concrete [1]. The compressive strength of EGC-G, EGC-M and EGC-P containing lightweight aggregates were 24%, 18% and 15%, respectively lower than that of EGC-S. This may be attributed to the fact that lightweight aggregates are usually weaker than micro-silica sand particles [11]. Among the four EGCs, the EGC-S mixture containing micro-silica sand exhibited the highest compressive strength, comparable to typical ECC M45. However, unlike typical ECC M45, EGC-S contains no cement, and therefore it has significantly lower environmental footprints compared to the typical ECC M45 in which its cement content is still 1.5 times that of normal concrete [9].

Material sustainability indicators (MSI) in terms of embodied energy and CO_2 emission were computed in this study to compare the material sustainability of EGC-S and typical ECC M45 [36]. Table 5 presents the mix proportions of EGC-S and typical ECC M45 and the life cycle inventory data of the ingredients. The inventory data was obtained from relevant literature [9,12,37–41]. It should be noted that three assumptions were made in deriving the life cycle inventory data given in Table 5. First, the embodied energy and CO_2 emissions associated with fly ash are zero as it is a by-product of coal power station, most of which is disposed in landfills. Second, the embodied energy and CO_2 emissions associated with water are negligible relative to other ingredients. Third, the embodied energy and CO_2 emissions associated with the heat curing approach (24 h at 60 °C) adopted for production of EGCs are derived from the data given in Yang et al. [40] and National Greenhouse Accounts Factors [41], considering the average emission factor for consumption of electricity from the grid in Australia to be 0.73 kg CO_2-e/kWh.

Fig. 1 presents the embodied energy and CO_2 emissions associated with production of a unit volume of EGC-S and ECC M45. The CO_2 emissions of EGC-S is 52% lower than that of ECC M45. This is mainly attributed to the replacement of OPC binder, which is highly energy and carbon intensive with fly ash-based geopolymer binder. On the other hand, the embodied energy of EGC-S is 17% lower than that of ECC M45. The reason for the relatively less reduction in the embodied energy associated with EGC-S over ECC M45 is the fact that although the embodied energy associated with fly ash is considered to be zero, however high embodied energy is still required for production of the activator solution and the heat curing approach adopted for the manufacture of EGC-S. It can be concluded that EGC-S is a promising sustainable alternative to ECC M45 in terms of carbon emission and energy consumption.

3.3. Uniaxial tensile performance

The uniaxial tensile stress–strain responses of the four green lightweight fly ash-based EGCs developed in this study are presented in Figs. 2–5. As observed in these figures, all lightweight EGCs, regardless of the aggregates, exhibited clear

Table 5 – Mix proportions of EGC-S and typical ECC M45 and life cycle inventory data of the ingredients used for calculating the MSI.

Ingredients	ECC M45[a] (kg/m^3)	EGC-S (kg/m^3)	Embodied energy (MJ/kg)	CO_2 emissions (kg/kg)
OPC	571	–	5.06[b]	0.898[b]
Fly ash	685	1029.7	–	–
Micro-silica sand	456	308.9	0.175[b]	0.026[b]
Water	332	–	–	–
Activator solution[c]	–	463.4	4.26[e]	0.358[d]
Superplasticizer	6.8	–	36.76[b]	1.48[b]
PVA fiber	26	26	106.54[b]	3.6[b]
Heat curing	N/A	Applicable	0.0828[f]	0.017[f]

[a] The mix proportion of typical ECC M45 is adopted from Yang et al. [9].
[b] Derived from Huang et al. [12] and Yang et al. [9].
[c] Refer to Section 2.1 for details of the activator solution.
[d] Derived from McLellan et al. [37].
[e] Derived from Fawer et al. [38] and Integrated Pollution Prevention and Control (IPPC) [39].
[f] Derived from Yang et al. [40] and National Greenhouse Accounts Factors [41].

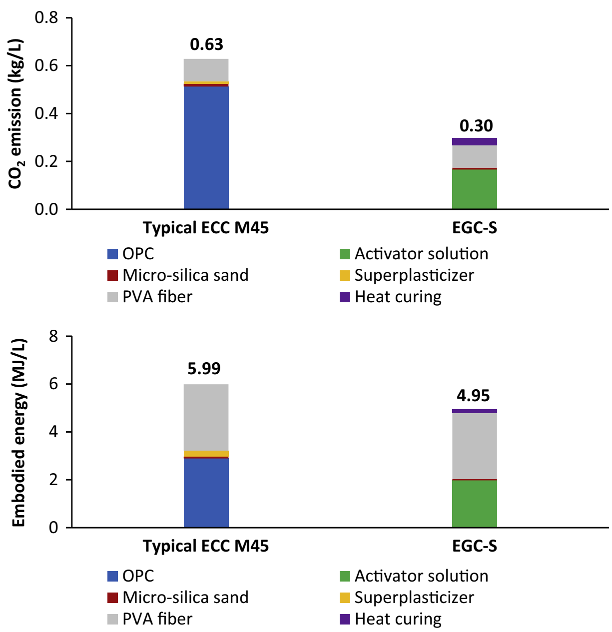

Fig. 1 – Material sustainability indicators of EGC-S and typical ECC M45.

pseudo strain hardening (PSH) behavior through multiple cracking process. The uniaxial tension test results including the average measured ultimate tensile strength (σ_{cu}) and tensile strain capacity (ε_{cu}) and the estimated first-crack strength (σ_{fc}) are presented in Table 6. The developed

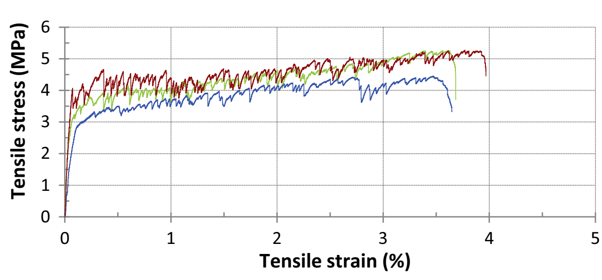

Fig. 2 – Tensile stress–strain responses of EGC-S.

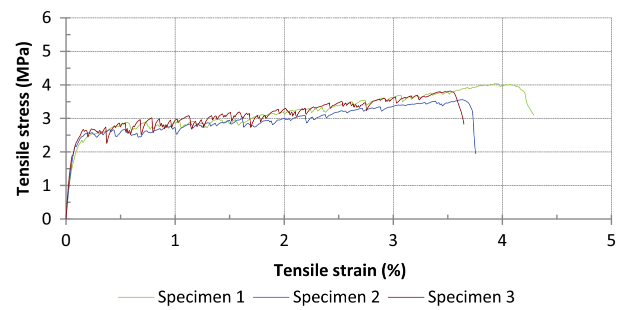

Fig. 3 – Tensile stress–strain responses of EGC-G.

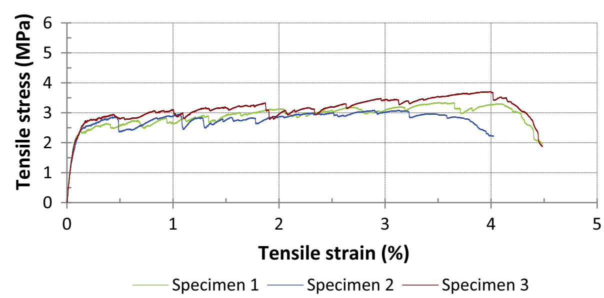

Fig. 4 – Tensile stress–strain responses of EGC-M.

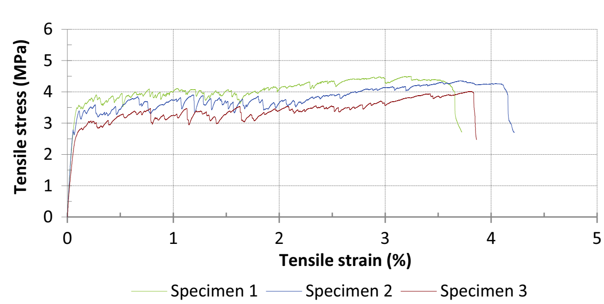

Fig. 5 – Tensile stress–strain responses of EGC-P.

lightweight EGCs exhibited moderate to high ultimate tensile strength in the range of 3.4–5.0 MPa. At the same time, they exhibited very high tensile strain capacity in the range of 3.5–3.7% which is about two orders of magnitude higher than

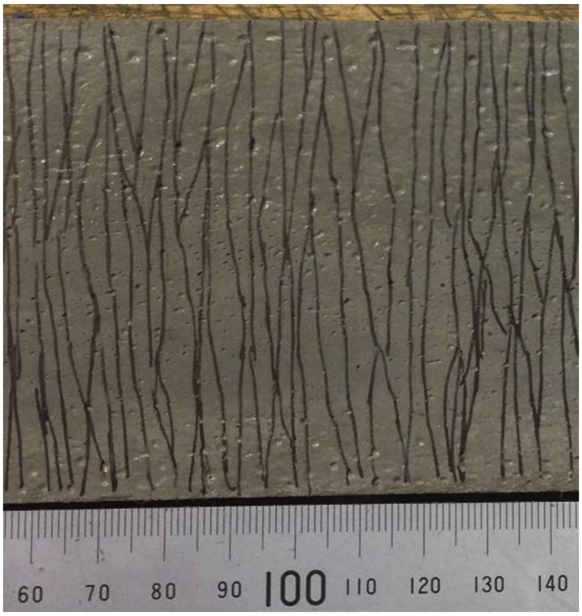

Fig. 6 – Crack pattern of EGC-S.

that of brittle OPC-based or geopolymer concrete. Therefore, the development of green lightweight EGCs with fly ash-based geopolymer as the sole binder is experimentally demonstrated.

Fig. 6 presents the crack pattern of EGC-S after unloading. The green lightweight fly ash-based EGC clearly shows the multiple-cracking behavior with uniform crack distribution and a narrow crack spacing of 2–3 mm representing saturated multiple cracking behavior, which corresponds to its significantly high tensile strain capacity. The average crack width of EGC-S under load is estimated to be approximately 100 μm based on the tensile strain capacity, the average crack spacing and the number of visible cracks. It should be noted that the actual crack width under load should be smaller than the estimated value of 100 μm because the actual number of micro-cracks formed during loading was more than the number of visible cracks after unloading as many micro cracks developed during loading completely closed after unloading, making them very difficult to be detected on the surface of the unloaded specimen [22,42]. Such a tight crack width indicates significant improvement in durability of green lightweight EGC compared to cracked brittle lightweight concrete with crack width at the scale of several hundred microns to a few millimeters [43].

As observed in Table 6, the first-crack strength of EGC-S and EGC-P, and that of EGC-G and EGC-M are comparable. The first-crack strength of EGC-S and EGC-P are about 30% higher than that of EGC-G and EGC-M due to their greater matrix fracture toughness [42]. This difference in matrix fracture toughness is likely due to the difference in the particle shape of the aggregates [10]. While the expanded recycled glass and hollow ceramic microspheres possess regular spherical shape [34,35], the micro-silica sand and expanded perlite particles are irregularly shaped [44,45]. The irregular shape of the aggregates increases the tortuosity of the fracture path along the interface between geopolymer paste and aggregates, thereby resulting in higher fracture toughness and first-crack strength of EGC-S and EGC-P than EGC-G and EGC-M [11].

According to Table 6, EGC-S containing normal weight micro-silica sand exhibited the highest ultimate tensile strength. The ultimate tensile strengths of EGC-G, EGC-M and EGC-P containing lightweight aggregates were 24%, 32% and 14%, respectively, lower than that of EGC-S. According to the micromechanics design theory of ECC, the ultimate tensile strength of the composite is governed by fiber bridging capacity, which is further affected by the fiber characteristics and fiber-matrix interfacial properties [11]. The lower ultimate tensile strength of the composites containing lightweight aggregates is likely due to their lower fiber-matrix bond. The relatively lower fiber/matrix frictional bond in EGC-G and EGC-M may be caused by the smooth spherical shape of the expanded recycled glass and hollow ceramic microspheres, compared to the irregularly shaped micro-silica sand and expanded perlite particles. Single fiber pullout tests and microscopic observations are needed to validate this explanation, which is outside the scope of this study.

The tensile strain capacities of EGCs are discussed below in terms of the two PSH performance indices proposed by Kanda and Li [46]. Adequate margins between maximum fiber bridging stress (σ_0) and first cracking strength (σ_{fc}) as well as complementary energy (J'_b) and crack tip toughness (J_{tip}) are required to obtain robust tensile ductility in the composite [47]. In order to be able to quantitatively evaluate these margins, Kanda and Li [46] proposed two PSH performance indices, namely stress-performance index (σ_0/σ_{fc}) and energy-performance index (J'_b/J_{tip}). It should be noted that the ultimate tensile strength (σ_{cu}) coincides with σ_0 of the composite when the composite exhibits the PSH behavior [48]. In theory, both PSH performance indices must at least exceed unity to obtain the PSH behavior in the composite. Higher PSH performance indices imply greater probability of saturated multiple cracking and greater tensile strain capacity of the composite.

According to Table 6, the tensile strain capacities of all EGCs, regardless of the aggregate, were about 3.5–3.7%. The stress-performance index of each composite reported in Table 6 for various EGCs is comparable (between 1.3 and 1.5). From Kanda and Li [46], stress-performance index greater than 1.2 typically leads to saturated multiple cracking. This condition is true for all sustainable lightweight EGCs in this study, and therefore leads to similar tensile strain capacity. This is one of the reasons for the comparable tensile strain capacity of the composites. The second reason is associated with the energy-performance index of the composites. The relatively lower ultimate tensile strength of EGC-G and EGC-M suggests that their J'_b could be lower than of EGC-S and EGC-P [49]. At the same time, the relatively lower first-crack strength of EGC-G and EGC-M indicates that their matrix fracture toughness and J_{tip} could be lower than those of EGC-S and EGC-P [11,42]. Therefore, it is hypothesized that although the J'_b of EGC-G and EGC-M could be lower than that of EGC-S and EGC-P, however due to their lower J_{tip}, their energy-performance index would be comparable to that of EGC-S and EGC-P. Therefore, as expected from micromechanics based design theory, it is not surprising that all sustainable lightweight EGCs in this study with comparable PSH performance indices exhibited comparable tensile strain capacities.

Table 6 – Uniaxial tension test results.

Mix ID	First-crack strength, σ_{fc} (MPa)	Ultimate tensile strength, σ_{cu} (MPa)	Tensile strain capacity, ε_{cu} (%)	Stress-performance index (σ_{cu}/σ_{fc})
EGC-S	3.4 ± 0.62	5.0 ± 0.47	3.6 ± 0.15	1.5
EGC-G	2.6 ± 0.09	3.8 ± 0.24	3.7 ± 0.22	1.5
EGC-M	2.5 ± 0.17	3.4 ± 0.32	3.5 ± 0.43	1.4
EGC-P	3.3 ± 0.27	4.3 ± 0.25	3.6 ± 0.30	1.3

3.4. *Thermal conductivity*

The thermal conductivity of concrete is typically sensitive to its moisture content. Greater moisture content results in greater thermal conductivity [50]. Although EGCs are not cement-based, their thermal conductivity also depends on the moisture content. Therefore, the thermal conductivity measurements should be performed at the same moisture content for all EGCs. In this study, all coupon specimens of various EGCs were at stable moisture content of 5.6% at the time of thermal conductivity measurements.

The thermal conductivities of all EGCs at ambient temperature (23 ± 3 °C) are reported in Fig. 7. The EGC-S containing normal weight micro-silica sand exhibited the highest thermal conductivity. The thermal conductivities of EGC-G, EGC-M and EGC-P containing lightweight aggregates were 49%, 38% and 40%, respectively, lower than that of EGC-S. The reduction in thermal conductivity of EGCs incorporating lightweight aggregates is attributed to the lower thermal conductivity of the lightweight aggregates than that of the normal-weight micro-silica sand [11]. The thermal conductivities of expanded recycled glass, ceramic microspheres, and expanded perlite are 0.07 W/(m K) [34], 0.10 W/(m K) [35], and 0.095 W/(m K) [45], respectively compared to 0.33 W/(m K) of dry silica sand [51]. According to Fig. 7, expanded recycled glass was the most effective in reducing the thermal conductivity among the lightweight aggregates used in this study, which is meaningful because the expanded recycled glass has the least thermal conductivity among various aggregates investigated in this study. The relatively lower thermal conductivity of expanded recycled glass is due to its multicellular structure [34]. It can be concluded that incorporation of lightweight aggregates can effectively reduce the thermal conductivity of the fly ash-based EGCs, which can potentially benefit energy conservation in buildings constructed with the green lightweight fly ash-based EGCs.

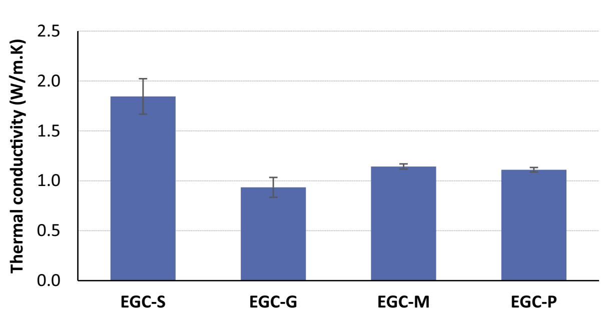

Fig. 7 – Thermal conductivities of sustainable lightweight fly ash-based EGCs.

4. Conclusions

This study presents the results of experimental determination of the mechanical and thermal properties of sustainable lightweight EGCs exhibiting significant strain hardening behavior under uniaxial tension. The influences of replacing normal weight micro-silica sand with three types of lightweight aggregates on the mechanical and thermal properties of the developed fly ash-based EGCs were experimentally evaluated. The sustainable lightweight fly ash-based EGCs developed in this study exhibited density of 1586–1833 kg/m^3, compressive strength of 43.4–56.8 MPa, thermal conductivity of 1.845–0.934 W/(m K), tensile strength of 3.4–5.0 MPa, and tensile strain capacity of 3.5–3.7%, depending on the type of aggregates. The following specific conclusions are drawn:

(1) The compressive strength and tensile performance of the fly ash-based EGC containing normal weight micro-silica sand (EGC-S) are comparable to those of typical ECC M45. At the same time, EGC-S is a cement-less and sustainable composite with 52% lower CO_2 emissions and 17% lower embodied energy compared to those of ECC M45. In addition, EGC-S with an average density of 1828 kg/m^3, unlike ECC M45 (2077 kg/m^3), can be classified as lightweight concrete.
(2) Among the lightweight aggregates investigated in this study, hollow ceramic microsphere was the most effective in reducing the density of the composite, with comparable tensile ductility and considerably (38%) lower thermal conductivity at the expense of 18% reduction in the compressive strength compared to those of the EGC containing normal weight micro-silica sand.
(3) The spherical shaped particles of expanded recycled glass and hollow ceramic microspheres cause reduction in the first-crack strength and ultimate tensile strength of the composite, compared to the EGCs containing irregularly shaped micro-silica sand and expanded perlite particles. This may be due to lower matrix fracture toughness and fiber-matrix interfacial bond, when spherical aggregates are used. The tensile ductility of all sustainable lightweight fly ash-based EGCs, regardless of the aggregate type, is very high (3.5–3.7%) due to high strength and energy performance indices resulting in saturated multiple cracking.
(4) Among the lightweight aggregates used in this study, expanded recycled glass was the most effective in reducing the thermal conductivity of the composite compared to the EGC containing normal weight micro-silica sand. It can be concluded that incorporation of lightweight aggregates can effectively (up to 49%) reduce the thermal conductivity of the composite, which can potentially reduce heat

exchange and total energy consumption in buildings constructed with the sustainable lightweight fly ash-based EGCs.

Acknowledgements

The authors gratefully acknowledge Kuraray Co. Ltd., Japan (PVA fibers), TGS Industrial Sand Ltd., Australia (micro-silica sand), Ausperl Pty Ltd., Australia (expanded perlite), Envirospheres Pty Ltd., Australia (hollow ceramic microspheres), Dennert Poraver GmbH, Germany and George Fethers & Co. Pty Ltd., Australia (expanded recycled glass) for providing materials used in this research. The first author would also like to acknowledge Swinburne University of Technology for the financial assistance in terms of a SUPRA scholarship for his Ph.D. study.

REFERENCES

[1] ACI 213R, ACI Committee 231. Guide for structural lightweight-aggregate concrete, 2014.
[2] S. Chandra, L. Berntsson, Lightweight Aggregate Concrete: Science, Technology and Applications, William Andrew Publishing, New York, 2002.
[3] S. Wang, V.C. Li, Lightweight engineered cementitious composites (ECC), in: Proceedings of 4th International RILEM Workshop on High Performance Fiber Reinforced Cement Composites (HPFRCC 4), vol. 1, 2003, 379–390.
[4] R. Hengst, R. Tressler, Fracture of foamed Portland cements, Cement and Concrete Research 13 (1) (1983) 127–134.
[5] M.H. Zhang, O.E. Gjvorv, Mechanical properties of high-strength lightweight concrete, ACI Materials Journal 88 (3) (1991) 240–247.
[6] J. Gao, W. Sun, K. Morino, Mechanical properties of steel fiber-reinforced, high-strength, lightweight concrete, Cement and Concrete Composites 19 (4) (1997) 307–313.
[7] S.B. Park, E.S. Yoon, B.I. Lee, Effects of processing and materials variations on mechanical properties of lightweight cement composites, Cement and Concrete Research 29 (2) (1999) 193–200.
[8] V.C. Li, H.-C. Wu, Conditions for pseudo strain-hardening in fiber reinforced brittle matrix composites, Applied Mechanics Review 45 (8) (1992) 390–398.
[9] E.-H. Yang, Y. Yang, V.C. Li, Use of high volumes of fly ash to improve ECC mechanical properties and material greenness, ACI Materials Journal 104 (6) (2007) 620–628.
[10] V.C. Li, T. Kanda, Innovations forum: engineered cementitious composites for structural applications, ASCE Journal of Materials in Civil Engineering 10 (2) (1998) 66–69.
[11] X. Huang, R. Ranade, Q. Zhang, W. Ni, V.C. Li, Mechanical and thermal properties of green lightweight engineered cementitious composites, Construction and Building Materials 48 (2013) 954–960.
[12] X. Huang, R. Ranade, V.C. Li, Feasibility study of developing green ECC using iron ore tailings powder as cement replacement, Journal of Materials in Civil Engineering 25 (7) (2012) 923–931.
[13] J.-K. Kim, J.-S. Kim, G.J. Ha, Y.Y. Kim, Tensile and fiber dispersion performance of ECC (engineered cementitious composites) produced with ground granulated blast furnace slag, Cement and Concrete Research 37 (7) (2007) 1096–1105.
[14] B. Nematollahi, J. Sanjayan, F.U.A. Shaikh, Synthesis of heat and ambient cured one-part geopolymer mixes with different grades of sodium silicate, Ceramics International 41 (4) (2015) 5696–5704.
[15] J. Davidovits, Geopolymers: inorganic polymeric new materials, Journal of Thermal Analysis 37 (8) (1991) 1633–1656.
[16] J.L. Provis, Modelling the formation of geopolymers, (PhD Thesis), Chemical & Biomolecular Engineering, University of Melbourne, 2006.
[17] B. Nematollahi, J. Sanjayan, Efficacy of available superplasticizers on geopolymers, Research Journal of Applied Sciences, Engineering and Technology 7 (7) (2014) 1278–1282.
[18] B. Nematollahi, J. Sanjayan, J.X.H. Chai, T.M. Lu, Properties of fresh and hardened glass fiber reinforced fly ash based geopolymer concrete, Key Engineering Materials 594 (2014) 629–633.
[19] Z. Li, Z. Ding, Y. Zhang, Development of sustainable cementitious materials, in: Paper Presented at the Proceedings of the International Workshop on Sustainable Development and Concrete Technology, 2004.
[20] P. Duxson, J.L. Provis, G.C. Lukey, J.S. Van Deventer, The role of inorganic polymer technology in the development of 'green concrete', Cement and Concrete Research 37 (12) (2007) 1590–1597.
[21] U.S. Department of Energy, Buildings energy data book, 2010 Retrieved from http://buildingsdatabook.eren.doe.gov/docs%5CDataBooks%5C2010_BEDB.pdf.
[22] B. Nematollahi, J. Sanjayan, F.U.A. Shaikh, Tensile strain hardening behavior of PVA fiber-reinforced engineered geopolymer composite, ASCE Journal of Materials in Civil Engineering 27 (10) (2015) 04015001.
[23] B. Nematollahi, J. Sanjayan, F.U.A. Shaikh, Strain hardening behavior of engineered geopolymer composites: effects of the activator combination, Journal of Australian Ceramic Society 51 (1) (2015) 54–60.
[24] B. Nematollahi, J. Sanjayan, F.U.A. Shaikh, Comparative deflection hardening behavior of short fiber reinforced geopolymer composites, Construction and Building Materials 70 (2014) 54–64.
[25] B. Nematollahi, J. Sanjayan, F.U.A. Shaikh, Influence of the type of activator combinations on the deflection hardening behavior of geopolymer composites, in: SHCC3 – 3rd International RILEM Conference on Strain Hardening Cementitious Composites, 3–5 November, Dordrecht, The Netherlands, RILEM Publications S.A.R.L., 2014 105–112.
[26] B. Nematollahi, J. Sanjayan, F.U.A. Shaikh, Influence of matrix related parameters on strain hardening behavior of engineered geopolymer composite (EGC), in: Concrete 2015 – The 27th Biennial National Conference of the Concrete Institute of Australia in Conjunction with the 69th RILEM Week Conference, 30 August–2 September, Melbourne, Australia, 2015.
[27] B. Nematollahi, J. Sanjayan, F.U.A. Shaikh, Matrix design of strain hardening fiber reinforced engineered geopolymer composite, Composites Part B: Engineering 89 (2016) 253–265.
[28] D.L. Kong, J.G. Sanjayan, Effect of elevated temperatures on geopolymer paste, mortar and concrete, Cement and Concrete Research 40 (2) (2010) 334–339.
[29] D. Hardjito, S.E. Wallah, D.M. Sumajouw, B.V. Rangan, On the development of fly ash-based geopolymer concrete, ACI Materials Journal 101 (6) (2014) 467–472.
[30] B. Nematollahi, J. Sanjayan, Effect of different superplasticizers and activator combinations on workability and strength of fly ash based geopolymer, Material and Design 57 (2014) 667–672.
[31] H. Okamura, K. Ozawa, Mix design for self-compacting concrete, Concrete Library JSCE 25 (6) (1995) 107–120.

[32] ASTM C109/C109 M, Standard test method for compressive strength of hydraulic cement mortars (using 50 mm [2 in.] cube specimens), ASTM Standards, United States, 2007.
[33] J. Cha, J. Seo, S. Kim, Building materials thermal conductivity measurement and correlation with heat flow meter, laser flash analysis and TCi, Journal of Thermal Analysis and Calorimetry 109 (1) (2011) 295–300.
[34] Poraver Technical Specifications [Online]. Dennert Poraver GmbH. Available: http://www.poraver.com/us/products/technical-data/ (accessed 20.02.15).
[35] E-SPHERES Technical Specifications [Online]. Envirospheres Pty Ltd. Available: http://www.envirospheres.com/products_bl.asp (accessed 10.02.15).
[36] V.C. Li, M. Lepech, S. Wang, M. Weimann, G. Keoleian, Development of green ECC for sustainable infrastructure system, in: Proceedings of International Workshop on Sustainable Development and Concrete Technology, Iowa State Univ., Ames, IA, (2004) 181–192.
[37] B.C. McLellan, R.P. Williams, J. Lay, A. Van Riessen, G.D. Corder, Costs and carbon emissions for geopolymer pastes in comparison to ordinary Portland cement, Journal of Cleaner Production 19 (9) (2011) 1080–1090.
[38] M. Fawer, M. Concannon, W. Rieber, Life cycle inventories for the production of sodium silicates, International Journal of Life Cycle Assessment 4 (4) (1999) 207–212.
[39] Integrated Pollution Prevention and Control (IPPC), Reference Document on Best Available Techniques in the Chlor-Alkali Manufacturing Industry, European IPPC Bureau, 2001.
[40] K.-H. Yang, J.-K. Song, K.-I. Song, Assessment of CO_2 reduction of alkali-activated concrete, Journal of Cleaner Production 39 (2013) 265–272.
[41] National Greenhouse Accounts Factors, The Department of the Environment – Australian Government, 2014. Retrieved from http://www.environment.gov.au/.
[42] V.C. Li, S. Wang, C. Wu, Tensile strain-hardening behavior of polyvinyl alcohol engineered cementitious composite (PVA-ECC), ACI Materials Journal 98 (6) (2001).
[43] V.C. Li, Reflections on the research and development of engineered cementitious composites (ECC), in: Proceedings of DFRCC-2002, Takayama, Japan, (2002) 1–22.
[44] TGS Industrial Sand Technical Specifications [Online]. T.G.S. Industrial Sands Pty. Ltd. Available: http://tgsindustrialsands.com.au/our-products/ (accessed 20.02.15).
[45] Ausperl Technical Specifications [Online]. Australian Perlite Pty Limited (AUSPERL) Available: http://www.australianperlite.com/perlite/ (accessed 20.02.15).
[46] T. Kanda, V.C. Li, Practical design criteria for saturated pseudo strain hardening behavior in ECC, Journal of Advanced Concrete Technology 4 (1) (2006) 59.
[47] E.H. Yang, V.C. Li, Strain-hardening fiber cement optimization and component tailoring by means of a micromechanical model, Construction and Building Materials 24 (2) (2010) 130–139.
[48] V. Li, D. Mishra, H.-C. Wu, Matrix design for pseudo-strain-hardening fiber reinforced cementitious composites, Materials and Structures 28 (1995) 586–595.
[49] B.Y. Lee, C.-G. Cho, H.-J. Lim, J.-K. Song, K.-H. Yang, V.C. Li, Strain hardening fiber reinforced alkali-activated mortar – a feasibility study, Construction and Building Materials 37 (2012) 15–20.
[50] R. Demirboğa, R. Gül, The effects of expanded perlite aggregate, silica fume and fly ash on the thermal conductivity of lightweight concrete, Cement and Concrete Research 33 (5) (2003) 723–727.
[51] C.J.M. Lasance, The thermal conductivity of silicon dioxide, Electronics Cooling August (2004).